Lessons Learned from Energy Storage System Demonstrations for Primary Frequency Control

Kwang-myung Yu[1][†], In-kyu Choi[1], Joo-hee Woo[1]

Abstract

In recent years, ESS (Energy Storage System) has been widely used in various parts of a power system. Especially, due to its fast response time and high ramp rate, ESS is known to play an important role in regulating grid frequency and providing rotational inertia. As the number of installed and commercially operating ESSs increases, the reliability becomes an important issue. This paper introduces control schemes and presents its test method for grid-connected ESS for primary frequency regulation. The test method allows to verify the control operation in the individual operation mode and state. A validation of the method through actual ESS test in a electrical substation is presented in the case study section.

Keywords: Energy Storage System, ESS, Primary Frequency Regulation, Frequency Control, Power System

I. INTRODUCTION

Traditionally, Korean power system have been operated by nuclear power plant and fossil fuel based generation sources, such as coal fired and gas power plants. However, as the global interest in Greenhouse Gas (GHG) reductions grows, there is a growing demand for green and Renewable Energy Sources (RES). The Korean government recently announced the "Implementation Plan for the 3020 Renewable Energy" [1] in order to achieve the GHG reduction target agreed through the 2015 Paris Climate Convention. According to the plan, the goal is to increase RES to 20% of total generation by 2030, which was 7% in 2016.

In power system operation, it is important to match the amount of power supplied with the amount consumed by the load. The power system operator must maintain a balance between demand and supply instantaneously.

The balance of supply and demand can be observed by measuring the frequency of the power system. Since Korean power system adopts the standard frequency as 60 Hz, If the supply and demand are exactly matched, the system frequency is measured as 60 Hz. If the power supply is greater than the demand (power generation>load), the grid frequency becomes greater than 60Hz. On the other hand, if supply is less than demand (power generation <load), the grid frequency becomes less than 60 Hz.

To maintain the grid frequency continuously near nominal value, it is necessary to secure spinning reserve. The Korean power system is securing 1,500 MW spinning reserve in accordance with the power system operating regulation of the KPX to prepare for the frequency fluctuation due to a contingency such as generation losses [2].

Fig. 2. shows a frequency response example of a power system after a large generation loss. The spinning reserve for frequency recovery consists of primary and secondary control reserves. Primary control reserve is configured on synchronous generators with slow response; response starts within 10 seconds. Therefore, the Rate Of Change Of Frequency (ROCOF) immediately after contingency is dependent on the inertia of the power system, not the amount of reserve. The inertia in a power system is defined as the inherent ability of synchronous machines to oppose sudden changes in generation or loss. This means that the size of ROCOF due to sudden imbalance in supply and demand is inversely related to the value of the inertia constant of a power system. In the future, if the inverter interfaced RES increase, the magnitude of the inertia of the system will be reduced, and the frequency fluctuation due to contingency will increase.

Battery Energy Storage Systems (BESS) have a fast charging/discharging response, and thus can be used as a reserve to mitigate frequency fluctuation in low inertia systems. The relationship of the frequency change due to supply and demand mismatch in a power system is expressed
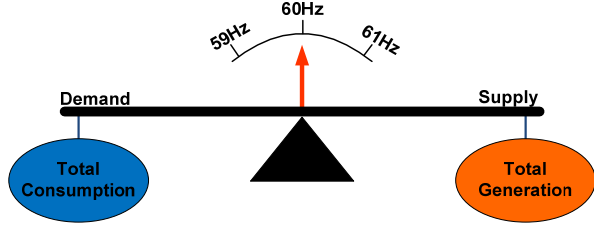
Fig. 1. Concept of frequency change due to power supply and demand mismatch.
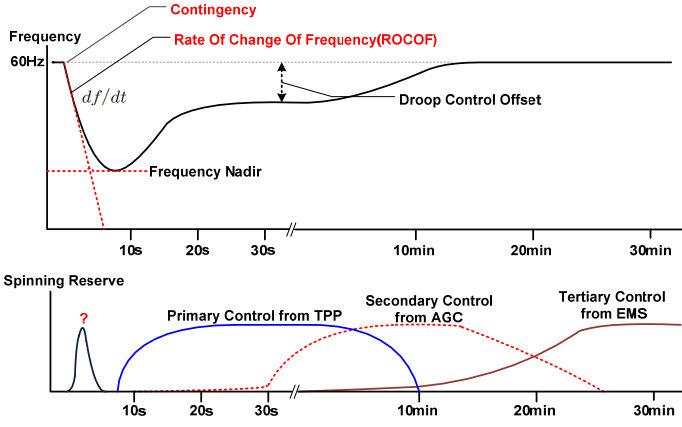
Fig. 2. Example of frequency response due to generation loss.

Fig. 3. Comparison of frequency response on different inertia and reserve speed [5].
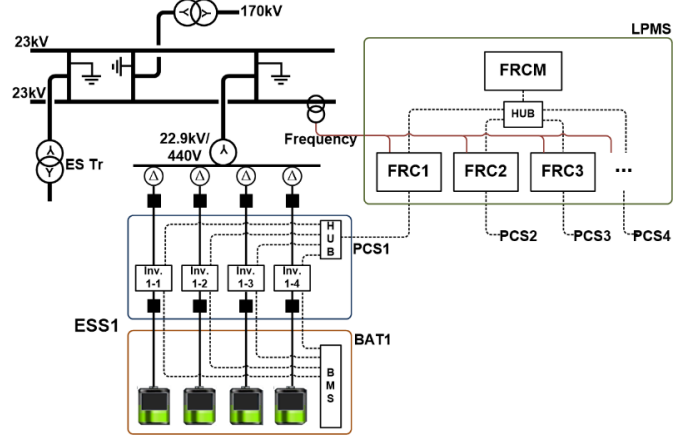
Fig. 4. ESS configuration connected to 22kV substation.

by the swing equation [3][4].

$$\Delta\dot{f} = \frac{f_0}{2HS_{rated}}(\Delta P_g - \Delta P_l - \Delta P_l^f) \qquad (1)$$

S_{rated} : Power system capacity (MW)
ΔP_g : Deviation in power generation (MW)
ΔP_l : Deviation in load (MW)
ΔP_l^f : Frequency dependent load deviation (MW)
f_0 : nominal frequency (Hz)
H : inertia constant (sec)

From the simulation results using above equation in Fig. 3., it can be seen that the blue line response with inertia of 3 seconds forms the lowest frequency (nadir frequency) at a lower point than the red line response with the inertia of 6 seconds for the same size of generation loss. In green response model, spinning reserve can be supplied immediately than the other two models since time constant of the spinning reserve is 1 second (T_t=1). The green line curve shows that the lowest frequency can be improved if the response time of reserve power is fast even with a small inertia value. The simulation results show that ESSs with fast response can play an important role in rotational inertia compentation in low inertia power systems.

In Korea, 2 pilot ESSs were installed, and currently, a total of 376 MW ESSs are in commercial operation at 13 substations. ESSs connected to a power system are likely to cause serious accidents in case of failure, so systematic system test and validation before commercial operation is required. In particular, verification of control algorithms, which are key to ESS operation, is essential for stable operation of ESS.
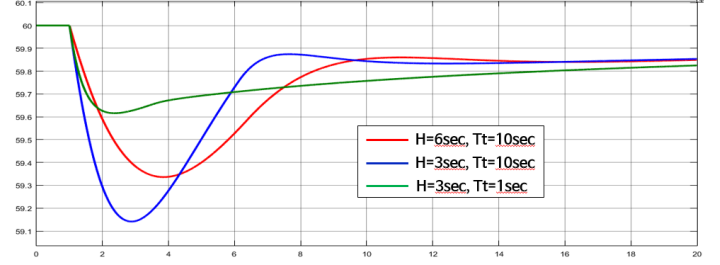
In this paper, we present a method for testing the control algorithm of ESS for primary frequency regulation. In order to implement the test, mimic frequency is injected to the controller, and the ESS target value generated by the controller is analyzed. The case study demonstrates that this method contributes to effective verification of control algorithms in each operation mode. This paper is organized as follows: Section II and III describe the ESS configuration and its primary frequency regulation algorithm. Section IV presents the test environment, and in Section V case studies are included. Conclusion is provided in Section VI.

II. ENERGY STORAGE SYSTEM ARCHITECTURE

ESSs in this study are installed in 22.9 kV substation and are connected to the grid through a 440 V/22.9 kV transformer. The ESS consists of a control system (Local Power Management System, LPMS), PCSs (Power Conditioning Systems), and battery & management systems. The PCS and battery system are installed separately in 4 MW /1 MWh units and are commanded by individual controller (Frequency Regulation Controller, FRC). LPMS consists of FRC for controlling individual PCS and battery system and FRCM (Frequency Regulation Controller Master) for balancing FRC outputs. This structure has an advantage in operating multiple PCSs and battery systems, and it facilitates capacity expansion. ESSs for primary frequency regulation installed in Korea are standardized with above structure.

III. FREQUENCY REGULATION ALGORITHM

This section describes the operating characteristics of the controllers configured in the LPMS. The LPMS consists of one FRCM and multiple FRCs for controlling individual inverters and battery sets [6].

A. FRC (Frequency Regulation Controller)

The FRC receives the system frequency and determines the operation mode. In addition, it calculates and transmits the charging/discharging target value for grid frequency control or battery SOC (State Of Charge) recovery to the inverter of PCS. There are three FRC operation modes as follows.

- Dynamic mode: entering for fast outage recovery and inertia support when the ROCOF of the grid exceeds the reference value
- Normal control mode: entering for frequency regulation when grid frequency deviates from normal range (dead band)
- Recharging mode: entering for battery SOC recovery when grid frequency is within the normal range

Fig. 5. shows the principle of FRC mode selection. To determine the operation mode, FRC receives the grid frequency, and it calculates the ROCOF and the magnitude of frequency deviation. As a first step, it is checked whether the ROCOF is less than a predetermined threshold value, $-\xi$. If the ROCOF is less than $-\xi$, FRC operates in dynamic mode. If ROCOF is not less than $-\xi$, secondly, FRC check the frequency deviation. In this step, if the frequency is within the stable range (normal range or dead band, $f_{db\,low} < f < f_{db\,high}$), the FRC operates in the recharging mode. In the opposite case, the FRC operates in the normal control mode.

1) Dynamic mode

The FRC enters the dynamic mode when the frequency suddenly falls due to contingency in the system such as a generation loss. In this mode, the FRC works to relieve ROCOF caused by the power system failure. Dynamic mode entry is determined as exceeding ROCOF reference value ($df/dt = -\xi$). Once in dynamic mode, it will not be released until the frequency enters the stable range. In this mode, the target value is calculated as follows.

$$FRC\ Target = K_d(f_0 - f) = K_d\Delta f \qquad (2)$$

K_d : System constant (MW/Hz)
f_0 : nominal frequency (Hz)
f : measured frequency (Hz)

The system constant K_d represents the relationship between the amount of power mismatch and frequency variation. In other words, it refers the amount of power required to change the grid frequency. Generally, the gain K_d in dynamic mode has a greater value than droop gain K_n in the normal control mode, which helps to inject power aggressively for the frequency drop.
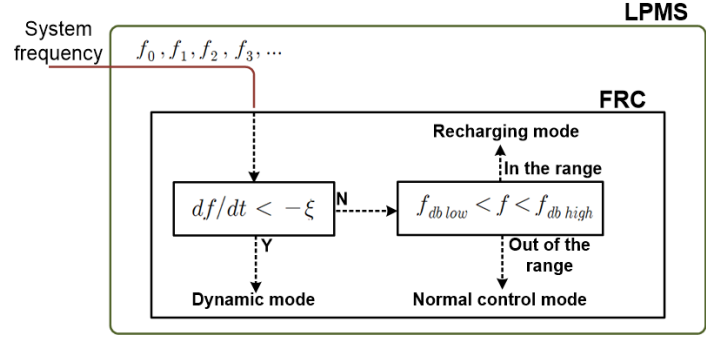

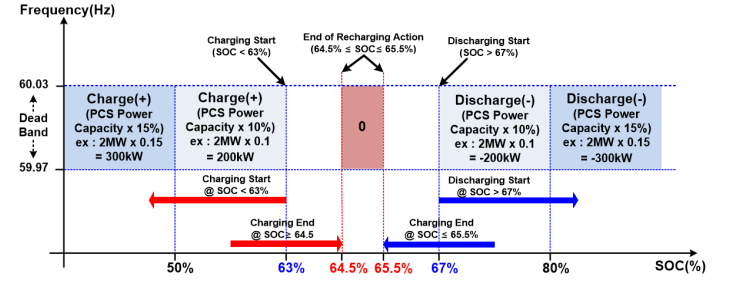Fig. 5. Concept of FRC operation mode selection.

Fig. 6. FRC operation scheme in the recharging mode.

2) Normal control mode

Although the frequency is not suddenly dropped, when the frequency deviates from the stable range ($f \leq f_{db\,low}$ or $f \geq f_{db\,high}$), it need be adjusted. In this case, the FRC enters the normal control mode and starts to regulate the frequency. In the normal control mode, the conventional droop control operation is implemented. The target is computed as follows.

$$FRC\ Target = K_n(f_0 - f) = K_n\Delta f \qquad (3)$$

$$K_n = \frac{\Delta P}{\Delta f} = \frac{P_{cap}}{f_0 \times R}$$
$$R = (\frac{\Delta f}{f_0})/(\frac{\Delta P}{P_{cap}})$$

K_n : gain (MW/Hz)
R : Droop
P_{cap} : Rated Power of PCS (MW)

3) Recharging mode

The FRC enters the recharging mode when the grid frequency is within the stable range.($f_{db\,low} < f < f_{db\,high}$) Since the ESS does not operate for frequency regulation in this mode, this stable range is also called dead band.

The ESS must charge extra energy from the grid when the power is oversupplied and provide energy when it is insufficient. Therefore, in the recharging mode, the target value is generated to ensure that the SOC is recovered near the midpoint.(ex: 65%) This helps ESS generate output bi-directionally when the FRC is operating in normal control mode in the future.

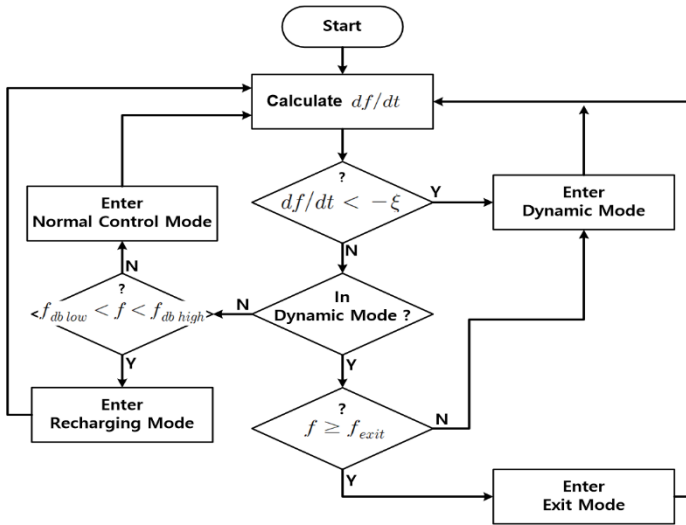If the SOC of the battery connected to each PCS is within
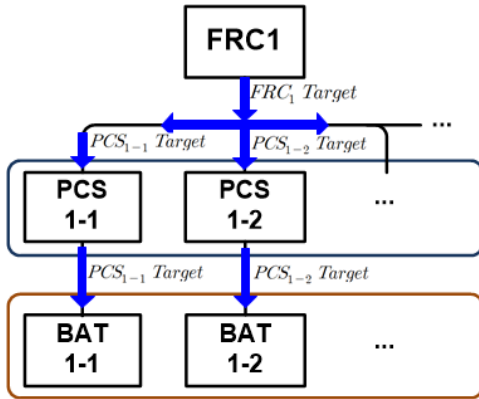
Fig. 7. Flow chart of FRC operation.

Fig. 8. FRC target distribution principle.

the range of 64.5~65.5% in the recharging mode, the charging/discharging operation is stopped. On the other hand, when the SOC is 63% or less, the charging operation starts. When the SOC is 67% or more, the discharging operation is performed. Recharging hysteresis between the starting point and the stopping point prevents the battery from shortening its service life due to frequent charge and discharge operations near the set point. When the SOC deviates significantly from the set point (50% or less, 80% or more), the charging / discharging power is increased (ex: rated power of PCS × 15%) and the SOC is rapidly recovered to the set point.

Fig. 7. presents a flow chart of FRC operation algorithm. At every time instance, FRC perform an operation according to the flow chart. At each time instance, the FRC calculates the ROCOF. If this value is less than $-\xi$, the FRC operates in the dynamic mode. Even if the ROCOF does not satisfy the dynamic mode entry criterion at the present time, if the grid frequency does not satisfy the exit mode entry criterion ($f \geq f_{exit}$), the dynamic mode operation is continuously performed. If the ROCOF does not satisfy the dynamic mode entry criterion and the FRC was not in the dynamic mode at the previous time, it operates in the normal control mode or the recharging mode according to the frequency deviation.

4) FRC target distribution

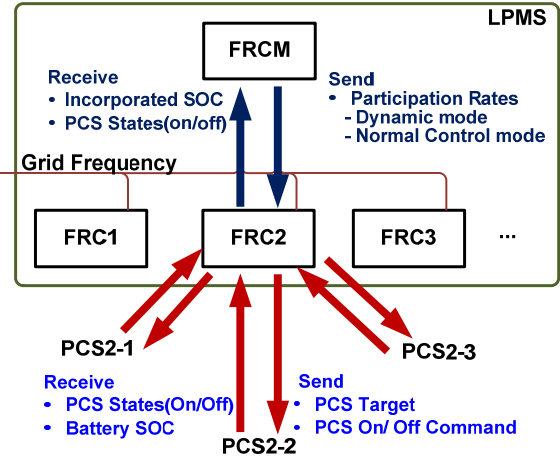One FRC manages multiple PCS modules (inverters) and

Fig. 9. Interaction between FRCM and FRC.

Table 1. Distribution weight (DW) of *PCSj* calculation formula in *nPCSs*

	Available SOC Range	$SOC_{CH\,Low} \sim SOC_{CH\,High}$
Charging	$DW_j = (100\% - SOC_j) / \sum_{i=1}^{n} (100\% - SOC_i)$	
	Available SOC Range	$SOC_{DSC\,Low} \sim SOC_{DSC\,High}$
Discharging	$DW_j = (SOC_j) / \sum_{i=1}^{n} (SOC_i)$	

battery sets. The FRC generates the target value according to the operation mode, and the distribution algorithm is executed so that the utilization of multiple batteries is balanced for this target command. For FRC target, target value distributed to each PCS is called PCS target. The distribution weight (DW) of each PCS is calculated by the SOC value of each corresponding battery. The PCS Target is calculated by multiplying the FRC Target by DW. For example, in Fig. 8., the target value of PCS 1-1 is calculated as follows.

$$PCS_{1-1}\,Target = FRC_1\,Target \times DW_{1-1} \qquad (4)$$

The DW is calculated differently depending on the state of charge and discharge. The formula is as shown in Table 1.

Table 1 shows that in order to keep the SOC of each battery at the same level, at charging state, the FRC target is more distributed to the PCS of the battery with low SOC than other PCS-batteries with higher SOC. At discharging, the FRC target is more distributed to the PCS of the high SOC battery. The sum of the PCS targets is the same as the FRC target. FRC target distribution algorithm operates in dynamic mode and normal control mode. There is an available SOC range that each battery can participate in charge/discharge operation. If the SOC of a battery is out of the range, it is excluded from the calculation. Therefore, the FRC target is only distributed between PCSs whose batteries' SOC are within the available SOC range.

B. FRCM (Frequency Regulation Control Master)

FRCM sends a participation rate to each FRC to balance the usage of each battery system of FRC. Based on the average SOC of the batteries connected to each FRC, FRCM calculates

Table 2. Normal control mode PR setting example

Condition	PR
$SOC_{low} \leq$ incorporated SOC of $FRC_j \leq SOC_{high}$	1
incorporated SOC of $FRC_j \leq SOC_{low}$ or incorporated SOC of $FRC_j \geq SOC_{high}$	0

* SOC_{low} : Incoporated SOC low limit for FRC Target generation
      SOC_{high}: Incoporated SOC high limit for FRC Target generation

the participation rate for dynamic mode and for normal control mode simultaneously at every time instance. The FRC takes both participation rates and selectively uses the participation rate depending on the corresponding operation mode. This participation rate is used as a weighting factor for the FRC target value or to determine whether the target value is generated or not. As a result, FRCM can prevent excessive use of certain FRC-batteries and helps keep average SOCs of each FRC-batteries even.

1) Dynamic mode participation rate
The participation rate of the dynamic mode is expressed by the weighting factor of each FRC target value. To calculate the participation rate, each FRCM receives incorporated (average) SOCs from each FRC, which are calculated as follows.

$$incorporated\ SOC\ of\ FRC_j = \sum_{i=1}^{n}(SOC_i)/n \qquad (5)$$

n: the number of batteries connected to FRC_j with PCS On

When calculating the incorporated SOC, only the batteries of the on-state PCS are considered. The dynamic mode participation rate (PR) of each FRC is computed as follows.

$$dynamic\ mode\ PR\ of\ FRC_j$$

$$= \frac{incorporated\ SOC\ of\ FRC_j}{\sum_{i=1}^{m}(incorporated\ SOC\ of\ FRC_i)} \qquad (6)$$

m: the number of FRC in LPMS

2) Normal control mode participation rate
The normal control mode participation rate determines whether the FRC target should be generated by referring to the incorporated SOC of the FRC. Therefore, the weighting factor of the normal control mode participation rate is 0 or 1.
Table 2. shows how to limit the target generation using the incorporated SOC range. Lithium Ion batteries, which are widely used for grid frequency control, show a tendency to shorten its service life under low or overcharge conditions. Therefore, this PR helps mitigate the shortening of the battery life by imposing restriction on the frequency regulation for the FRC having the out of available incorporated SOC range.

IV. CONTROL ALGORITHM TEST ENVIRONMENT

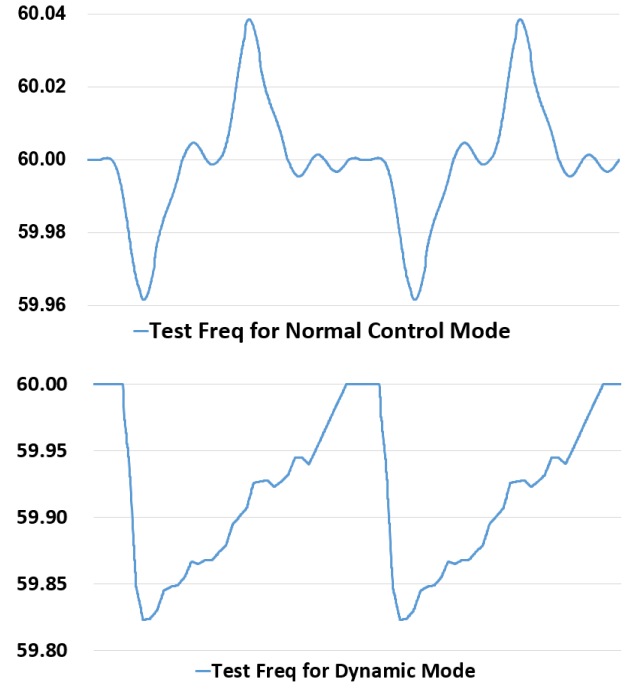After ESS installation or system upgrade, commissioning
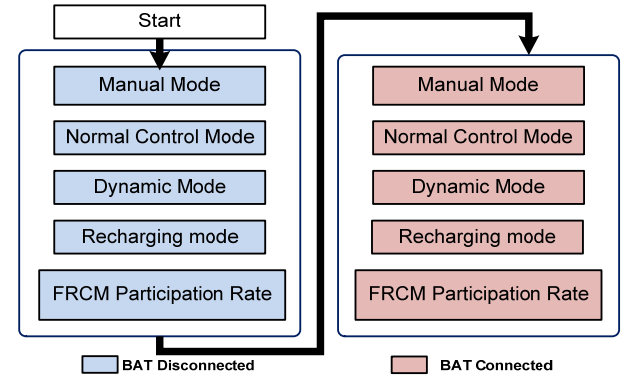

Fig. 11. Test frequency.

Fig. 12. Control algorithm test procedure.

is carried out to verify that the system is operating properly. At this time, the control algorithm verification process also proceeds. The LPMS has a setting unit that can inject the test frequency and virtual SOC so that the algorithm can be tested at any time in the field.

When testing the algorithm, instead of the actual grid frequency, the test frequency and virtual SOC in the test setting unit are injected into the FRC. Then the target value is checked to see if the FRC is in appropriate operation.

The test frequency consists of one for normal control mode verification and another one for dynamic mode verification, and each frequency waveform has been developed so that operation characteristics can be analyzed clearly.

Fig. 12. Shows the ESS control algorithm test procedure. The test consists of battery disconnection test and battery connection test. The test items in disconnection and connection test are the same, which are manual mode, normal control mode, dynamic mode, recharging mode, and FRCM participation rate test. The following section introduces each test item based on actual cases.

Table 3. Gimje substation ESS specification [7]

Location	Controller		PCS		Battery	
	Supplier	Model	Supplier	MW	Supplier	MWh
Gimje-si, Korea	GE	PAC System	Hyosung	48	LG Chem.	12

Table 4. FRC parameters for Gimje S/S ESS [7]

Variables	Description	Value
f_0	Norminal Frequency (Hz)	60
f	Measured frequency (Hz)	-
$f_{db\,low}$	Frequency stable range lower limit (Hz)	59.97
$f_{db\,high}$	Frequency stable range upper limit (Hz)	60.03
ξ	Dynamic mode threshold (Hz/sec)	0.028
f_{exit}	Exit mode threshold frequency (Hz)	59.9
P_{cap}	Rated power of PCS for each FRC (MW)	4
R_n	Droop in normal control mode	0.00279
R_{exit}	Droop in exit mode	0.0016
K_d	FRC target gain in dynamic mode (MW/Hz) $FRC\ Target = K_d(f_0 - f) = K_d\Delta f$	7,870
K_n	FRC target gain in normal control mode (MW/Hz) $K_n = \dfrac{\Delta P}{\Delta f} = \dfrac{P_{cap}}{f_0 \times R_n}$ $FRC\ Target = K_n(f_0 - f) = K_n\Delta f$	23.895
K_{exit}	FRC target gain in exit mode (MW/Hz) $K_{exit} = \dfrac{\Delta P}{\Delta f} = \dfrac{P_{cap}}{f_0 \times R_{exit}}$ $FRC\ Target = K_{exit}(f_0 - f) = K_{exit}\Delta f$	41.667
$SOC_{CH\,Low}$	Available SOC range lower limit in charging and normal control mode (%). Refer to table 1.	0
$SOC_{CH\,High}$	Available SOC range upper limit in charging and normal control mode (%). Refer to table 1.	80
$SOC_{DSC\,Low}$	Available SOC range lower limit in discharging and normal control mode (%) Refer to table 1.	50
$SOC_{DSC\,High}$	Available SOC range upper limit in discharging and normal control mode (%). Refer to table 1.	100

V. CASE STUDY

We now show how the test environment and method can be used for real grid-connected ESSs. In order to validate the effectiveness, we investigate test result of 48 MW ESS in Gimje substation located central part of Korea Republic [7].

The FRC parameters in Table 4 are used for the test.

A. Manual mode test

In the manual mode test, it is verified whether the correct target value is delivered to the PCS when the FRC target is manually entered. If the battery response reaches within 200 ms after the target command is input, it is recognized that the criterion is satisfied. In order to verify in various target ranges, the discharge response is checked while increasing the step input target in units of 100 kW, and the charging response is also checked in the same manner. Fig. 13. shows a manual mode test result for one FRC, where the negative target value represents discharge and the positive value represents charge.

B. Normal control mode test

Two tests are conducted using the same test frequency in the normal control mode test. In the first test, the SOC of each PCS-battery is set to the same value by the virtual SOC setting function. This test is to ensure that the FRC performs
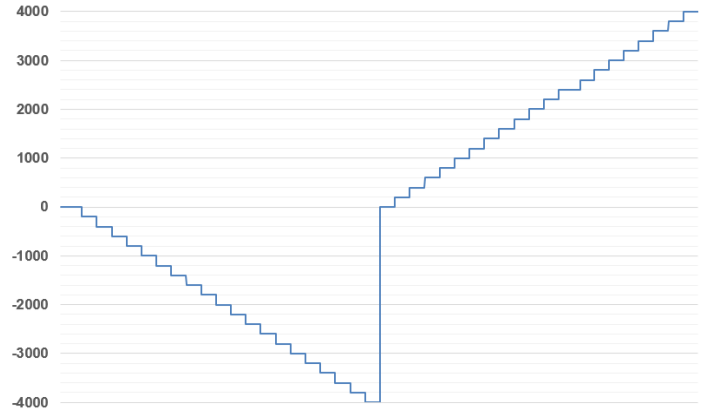

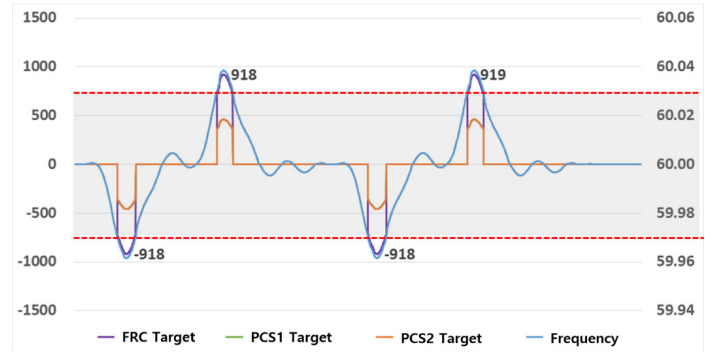Fig. 13. Manual mode test result (FRC No. 1).

Fig. 14. Normal control mode test result with the same SOC settings (65%, FRC No. 1).

the target operation correctly for the input frequency. In the second test, the SOC of each PCS-battery is set to a different value to confirm PCS target distribution.

1) Normal control mode test with the same SOC settings

Fig. 14. shows the results of the normal control mode test of one FRC. The SOCs of the batteries #1 and #2 were set to 65% respectively. From this result, it can be seen that when the frequency deviates from the deadband between the red dashed lines, it enters the normal control mode and generates a target value for frequency regulation. Since the SOC of each battery is set to the same value of 65%, the FRC target is equally distributed to each PCS in half.

2) Normal control mode test with the different SOC settings

Fig. 15. shows the result of the normal control mode test when the SOC setting of each PCS-battery is different. In the first cycle of the test frequency, the SOCs of each battery are set to 45 and 85%, and in the second cycle, they are set to 60 and 70%. In the first cycle 1-1 region, the FRC target was -919 kW due to the frequency deviating from the deadband. In this region, the SOC of the PCS-battery 1 is set to 45%, and the PCS1 is excluded from the battery discharge operation. (Normal control mode available SOC range for discharging: 50~100%, refer to Table 4.) Therefore, PCS2 will accommodate the entire FRC target value.

$$FRC\ Target = K_n(f_0 - f) = PCS2\ Target \qquad (7)$$

On the other hand, in the 1-2 region, the frequency

deviates from the deadband upper limit resulting in the FRC target 919 kW. In this region, PCS2 is excluded from the charging operation and PCS1 accepts the entire FRC target. (Normal control mode available SOC range for charging: 0~80%, refer to Table 4.)

$$FRC\ Target = K_n(f_0 - f) = PCS1\ Target \tag{8}$$

In the second frequency cycle, both SOC settings of the two PCS-batteries are within the operating range. Thus, the two PCSs have nonzero target values. In the area 2-1, PCS1 and PCS2 target values are distributed as follows according to the discharge value distribution formula.

$$PCS1\ Target = 60/(60+70) \approx 0.46 FRC\ Target \tag{9}$$

$$PCS2\ Target = 70/(60+70) \approx 0.54 FRC\ Target \tag{10}$$

In the area 2-2, the PCS1 and PCS2 target values are distributed according to the charge value distribution formula.

$$PCS1\ Target = \frac{100-60}{\{(100-60)+(100-70)\}} \approx 0.57 FRC\ Target \tag{11}$$

$$PCS2\ Target = \frac{100-70}{\{(100-60)+(100-70)\}} \approx 0.43 FRC\ Target \tag{12}$$

C. Dynamic mode test

Similar to the normal control mode test, the dynamic mode test consists of two sub-tests. In the first test, the SOC of each PCS-battery is set to the same value. This test is to ensure whether the FRC enters the dynamic mode according to the ROCOF and whether the target operation is performed properly. In the second test, the SOC is set differently to verify that the PCS target distribution in the dynamic mode is correct.

1) Dynamic mode test with the same SOC settings

Fig. 16 shows the dynamic mode test result of one FRC. If the absolute value of ROCOF is greater than ξ, the FRC enters the dynamic mode and its FRC Target is the value obtained by multiplying the frequency deviation by the system constant K_d as shown in the following equation.

$$FRC\ Target = K_d(f_0 - f) = K_d \Delta f \tag{13}$$

The system constant used in this test is 7,870,000 kW/Hz, which is much larger than the gain in the normal control mode. The rating of each PCS is 2 MW, and the battery capacity connected to each PCS is 0.5 MWh. When the FRC enters the dynamic mode due to the test frequency, a large FRC target is calculated. If FRC target is larger than sum of each PCS rating, the target delivered to each PCS is saturated with the PCS maximum output (2 MW).
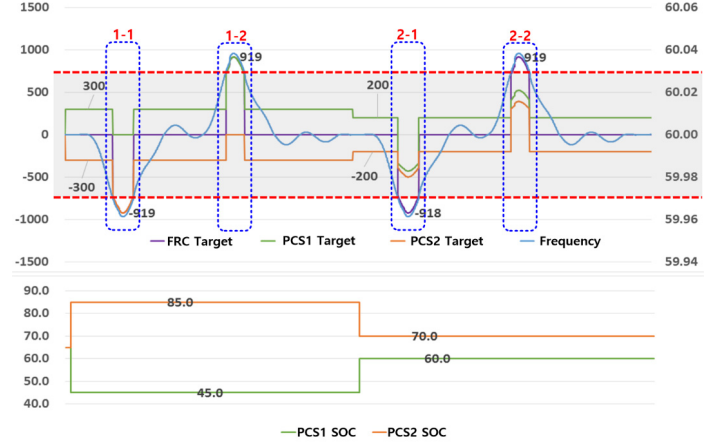

Fig. 15. Normal control mode test result with the different SOC settings (FRC No. 1).
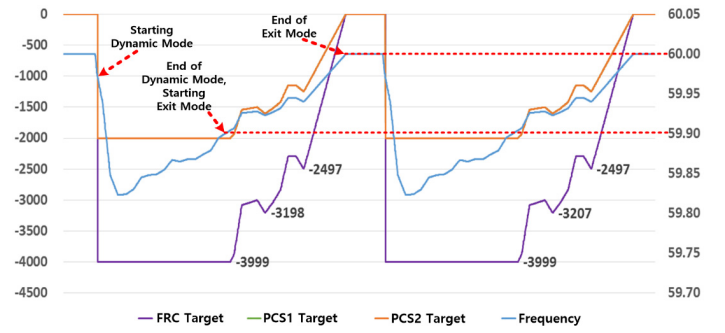

Fig. 16. Dynamic mode test result with the same SOC settings (65%, FRC No. 1).

$$PCS1, 2\ Target = max\left(FRC\frac{Target}{2}, 2\ \text{MW}\right) \tag{14}$$

When the grid frequency recovers to more than f_{exit}=59.9 Hz, the FRC exits the dynamic mode and switches to the exit mode. Each PCS target at this mode is as follows.

$$FRC\ Target = K_{exit}(f_0 - f) = K_{exit}\Delta f \tag{15}$$

$$PCS1, 2\ Target = max(\frac{K_{exit}\Delta f}{2}, 2\ \text{MW}) \tag{16}$$

where $K_{exit} = \frac{\Delta P}{\Delta f} = \frac{P_{cap}}{f_0 \times R_{exit}}$

2) Dynamic mode test with the different SOC settings

In Fig. 17, the target response of each PCS in dynamic mode is shown when the SOC of each battery is different. In the first cycle of the test, the SOC of each battery connected to PCS1, 2 was set to 9% and 92%, respectively. In dynamic mode, however, the PCS only operates when the connected battery SOC is in the range of 10 to 100%. Therefore, the target of PCS1 set to SOC 9% becomes 0, only PCS2 target is computed to maximum power rating 2 MW. In the second frequency cycle, the SOC of PCS1, 2 is set to 60% and 70%, respectively. Since all of these values are included in the dynamic mode operating range, both PCS1 and 2 targets are generated.
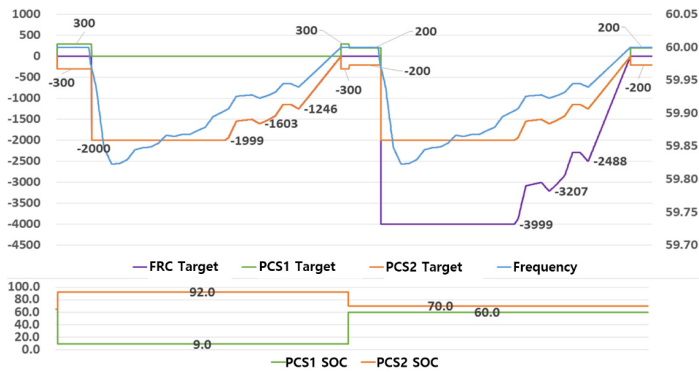
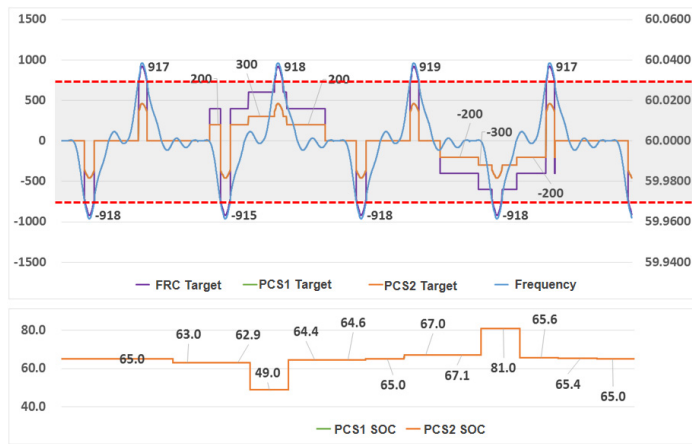Fig. 17. Dynamic mode test result with the different SOC settings (FRC No. 1).

Fig. 18. Recharging mode test result.

D. Recharging mode test

In the recharging mode test, it is verified whether the FRC generates the proper target to restore the battery SOC to the set value when the grid frequency is located within the deadband. The recharging algorithm has a hysteresis between recovery start and stop points to prevent shortening of battery life due to frequent charging and discharging near the battery SOC set point. Therefore, this test focuses on whether recovery targets are generated as expected near the hysteresis.

For the recharging mode test, the SOCs of each battery are set as in Fig. 18. The SOCs are initially set to 65% and the value changes sequentially. (65.0 → 63.0 → 62.9 → 49.0 → 64.4 → 64.6 → 65.0 → 67.0 → 67.1 → 81.0 → 65.6 → 65.4 → 65.0) The test frequency is injected with the same as the normal control mode test frequency. However, in this test, the primary objective is to verify the recharging behavior when the test frequency is within the dead band. According to Fig. 17, when the frequency is within the dead band, no

recharging action is taken even if the SOC is reduced to 63% after the battery SOC is initially set at 65%. After this, when the SOC is changed to 62.9%, the FRC generates the charging target of 200 kW (2 MW PCS rating×10%) for each PCS. The when the SOC is set to 49%, the FRC compute a charging target of 300 kW (3 MW PCS rating×10%) for each PCS. This target value is maintained until the SOC is increased to 64.4%, and the charging recovery is stopped when the SOC is increased to 64.6%. Thereafter, recovery of the SOC set value through discharging proceeds similarly.

VI. CONCLUSIONS

In this paper, we have shown a systematic test method for grid connected ESSs for primary frequency control. In order to do so, test frequency and virtual SOC setting units are injected to controllers, targets generated by controllers are compared with expected values. The proposed method confirms whether the target is properly generated based on the operating characteristics of the individual operation mode. The test results applied to the actual ESS demonstrate that the proposed method can improve reliability by eliminating computational errors that may occur during commercial operation.

REFERENCES

[1] "Implementation Plan for the 3020 Renewable Energy", Ministry of Trade, Industry and Energy, 2017.
[2] "Power System Operation Regulation," KPX, 2017.
[3] P. Kundur, "Power System Stability and Control", McGraw-Hill Inc., New York, 1994.
[4] P. M. Anderson, A. A. Fouad, "Power System Control and Stability", 2nd Edition, A john Wiley & Sons, 2003.
[5] K. M. Yu, "The Need of ESS for Frequency Control due to the Increase of Renewable Energy Sources", KIEE Electricity World, Vol. 67, No.3, 2018, pp.24-29.
[6] "Development of Control Algorithm of ESS for Frequency Regulation in Power System", Korea Electric Power Corporation Research Institute, 2015.
[7] "Gimjae 40MW FR ESS Test Report", Korea Electric Power Corporation Research Institute, 2017.
[8] A Oudalov, D Chartouni, C Ohler, "Optimizing a Battery Energy Storage System for Primary Frequency Control", IEEE Transactions on Power Systems 22 (3), 2007, pp. 1259-1266.
[9] A. Ulbig, T.S. Borsche, G. Andersson, "Impact of Low Rotational Inertia on Power System Stability and Operation", IFAC 2014 Proc Vol. 47, 2014, pp.7290-7297.